communications physics

Article

https://doi.org/10.1038/s42005-024-01826-z

Modeling photomolecular effect using generalized boundary conditions for Maxwell equations

Gang Chen

We recently demonstrated via experiments in hydrogels and at a single air-water interface the photomolecular effect: photons directly cleaving off water molecular clusters in the visible spectrum where bulk water has negligible absorption. To model single interface experiments, here we re-derive generalized boundary conditions for Maxwell equations by assuming a transition region of the electromagnetic fields across the interface, leading naturally to the Feibelman parameters used before to describe surface photoelectric and surface plasmon effects on metals. This generalization leads to modifications of the Fresnel coefficients and an expression for the surface absorptance that can reasonably explain trends in our single-interface experimental data on the angle and polarization dependence of the beam deflection. Our work provides further support for the existence of the photomolecular effect, suggests that surface absorption should exist in many materials, and lays a foundation for assessing the impacts of such surface absorption based on the Maxwell equations.

Based on a series of experiments, we recently demonstrated that visible light can directly cleave off water molecular clusters from water-air interfaces despite bulk water absorbs very little in the visible spectrum, and we called this process the photomolecular effect[1,2]. Our experimental observations were first made based on water evaporation from porous hydrogel and then from a single air-water interface under sunlight, light-emitting diodes (LEDs), and laser irradiation. The photomolecular effect was introduced to explain the super-thermal evaporation rates observed[3,4] in some solar interfacial-evaporation experiments: evaporation from porous materials floating on water surface subjected to sunlight irradiation[5–7]. The photomolecular effect is surprising and poses challenges for modeling, from both microscopic and macroscopic perspectives. Microscopically, the details of water cluster cleavage processes remain unclear. Macroscopically, the question is how we can model the process based on the Maxwell equations. This paper focuses on answering the latter question, which is important for simulating absorption of clouds and hydrogels due to the photomolecular effect.

Although a microscopic model for the photomolecular effect is still lacking, we conceived the photomolecular effect[1,2] based on the insights illustrated in Fig. 1a. One insight is the implications of the continuity of the displacement field of the electromagnetic wave perpendicular to the interface as required by the Maxwell equations, i.e., $\varepsilon_1 E_{z1} = \varepsilon_2 E_{z2}$, where $\varepsilon_1 = 1$ for air and $\varepsilon_2 = 1.8$ for water in the visible spectrum, and the subscript "z" is the coordinate direction perpendicular to the interface[8,9]. This condition means that the electrical field in the perpendicular direction is reduced by nearly a factor of two from air to water across the interface which is only ~3 angstroms in thickness[10,11], creating a large gradient of the electric field. Another insight is that water molecules are polar and form fluctuating hydrogen bond networks, also called water clusters[12,13]. These two facts mean that the change of the electric field over the distance of a single water cluster at the interface is appreciable, leading to a net force exerted on the molecular clusters and pulling them from the interfacial region to the adjacent free space [Fig. 1a]. This process is similar in some ways to the surface photoelectric effect, also due to the large electric field gradient across the interface where electron density changes within 1–2 Å[14,15].

There are, of course, significant differences between the surface photoelectric effect and the photomolecular effect we hypothesized. The former is the ejection of electrons while the latter is the ejection of the water molecular clusters which can be ~10^5 times heavier. We hypothesize that a single photon can meet the energy and momentum conservation requirements underpinning the photomolecular effect: as water molecules have ~1.5 hydrogen bonds with a bond energy ~0.24 eV, much smaller than that of a photon in the visible spectrum[16]. Although the momentum of a single photon is very small, the steep change of the electrical field at the interface provides additional spatial momentum. However, one can still question the detail process: (1) why can this process happen in a spectral region when essentially no absorption occurs inside the bulk material? and (2) how can a water molecular-cluster be ejected from surface. For question (1), I believe that the empty space above the surface provides final states for the water molecular clusters which do not exist inside the bulk material. It is harder to

Department of Mechanical Engineering, Massachusetts Institute of Technology, Cambridge, MA, USA. e-mail: gchen2@mit.edu

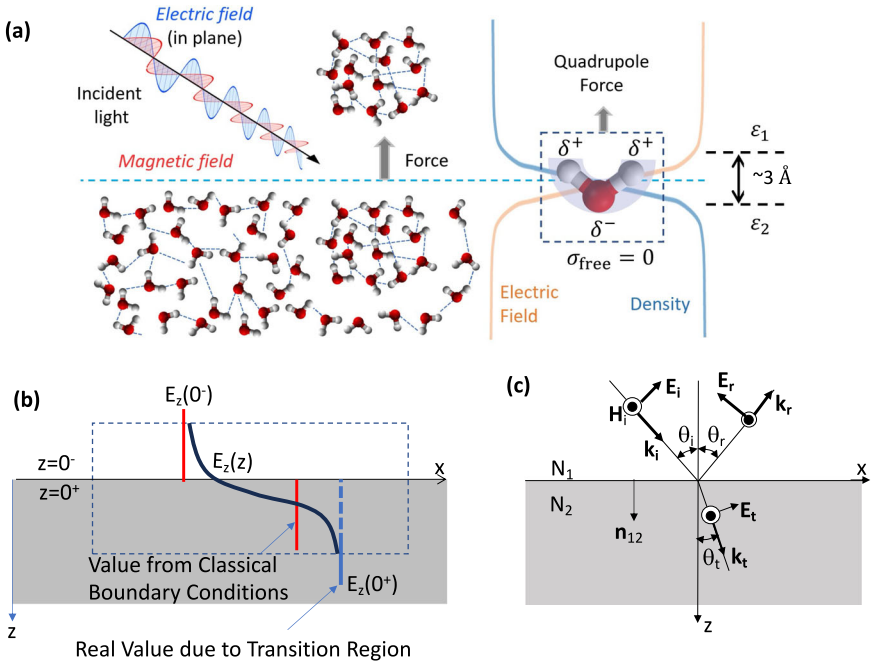

Fig. 1 | Illustrations of physical pictures. **a** Illustration of the photomolecular effect and its driving force. At an air-water interface, the perpendicular components of the displacement fields created by an incident electromagnetic field are continuous according to the classical boundary conditions for the Maxwell equations, implying a large electric field gradient over water clusters at the interface and hence a non-zero force to knock out these clusters. **b** Basic ideas in modifying Maxwell equations' boundary conditions. The continuity of the displacement fields means that the electric field changes abruptly across the interface, as represented by the two red-lines. In reality, the electrical field changes rapidly but continuously across the interface, as represented by the black line. Including such a continuously-changing picture leads to a different value of the electric field across the interface, which when extended back to zero-thickness interface becomes $E_z(0^+)$ as represented by the blue line. **c** Coordinate system used in deriving the modified Fresnel coefficients for reflection and transmission of an incident beam.

answer question (2). The bulk photoelectric process on electrons involves excitation of an electron to higher energy level by a photon, transport to surface and tunnel to vacuum. The surface photoelectric process on electrons also involves multimode surface plasmons[14]. Water does not support surface plasmons[17,18]. We can imagine that the steep gradient at the interface first distorts the electron distribution in the permanent dipoles, which transfers to the nuclei and starts a cascade event that eventually drives out the water molecular clusters. Clearly, much remains to be done to really understand the microscopic mechanisms behind the photomolecular effect.

In this paper, we rederive the generalized boundary conditions for the Maxwell equations built on the Feibelman parameters, which were developed to describe responses of metal surfaces to light[14,15]. These boundary conditions lead to modifications of the Fresnel reflection and transmission coefficients, and a new expression for interfacial absorptance. For non-absorbing substrates, the interfacial reflectance, transmittance, and absorptance are dependent only on the imaginary parts of the Feibelman parameters. We show that the interfacial absorptance expressions capture the angle and polarization trends observed in the photomolecular effect, hence lending confidence to the photomolecular effect in addition to establishing a foundation to simulate the effect. Our work also suggests that surface absorption is a universal process and can be modeled with the Feibelman parameters.

Results

Macroscopic approaches: generalized boundary conditions for Maxwell equations

Despite lack of a microscopic model at this stage, we can still develop ways to model the surface absorption process underlying the photomolecular effect. There are two main approaches to describe the surface absorption phenomena. One is adding another layer between the two media[19] and the other is treating the surface region fields as nonlocal with nonlocal dielectric constants[14]. In the first approach[19], also called the three-phase model, Taylor expansion is used to simplify the reflection coefficient for the film-on-a-substrate configuration since the interfacial film thickness is generally much smaller than the wavelength, arriving at simplified expressions for the differential change of the surface reflectance and absorptance. This approach was widely used in differential surface reflectance spectroscopy and surface absorption spectroscopy to analyze adsorbed surface layers during thin film growth[20–22] and electrochemical reaction at metal-electrolyte interfaces[23].

Although the three-phase model treated the interfacial region as a thin layer with well-defined macroscopic dielectric constant and thickness, the discontinuities implied in the traditional boundary conditions for the Maxwell equations never really happen even in the absence of an intermediate layer. In reality, the electric field changes rapidly but continuously over a short distance. In this region, the dielectric constant is nonlocal. For example, in the coordinate system as shown in Fig. 1b, the displacement field is $\boldsymbol{D}(\boldsymbol{r}) = \int \overleftrightarrow{\varepsilon}(\boldsymbol{r}, \boldsymbol{r}')\boldsymbol{E}(\boldsymbol{r}')d\boldsymbol{r}'$, where $\overleftrightarrow{\varepsilon}$ is the nonlocal dielectric tensor in the interfacial region, which means that the displacement at $\mathbf{r}$ is affected directly by the electrical field in the entire transition region. Different models for the nonlocal response at the interfacial region for electrons had been developed[14,15,24–30]. Among them, Feibelman's approach by combining the density functional theory solution for the electron distribution with the microscopic Maxwell equations, assuming a jellium model of electrons at the interface, is considered the most accurate. The detailed simulation results can be summarized into two surface response functions, called the Feibelman parameters, $d_{\parallel}(\lambda)$ and $d_{\perp}(\lambda)$, which can be used to form a set of generalized boundary conditions for the Maxwell equations, which had been derived before[14,31–34].

Although all previous discussions of the Feibelman parameters were based on light interactions with electrons at a metal surface, the derivation of the generalized boundary conditions from the Maxwell equations requires no such background. As long as we recognize that the transition of the electric field between the two sides of the interface occurs over a small distance continuously [Fig. 1b], the generalized boundary conditions naturally emerge when one integrates over a spill-box spanning the transition region, as we show in the Methods section. These conditions are[32,34]

$$[\![\boldsymbol{H}_{\parallel}]\!] = i\omega d_{\parallel}[\![\boldsymbol{D}_{\parallel}]\!] \times \boldsymbol{n}_{12} \tag{1}$$

$$[\![\boldsymbol{D}_{\perp}]\!] = d_{\parallel}\nabla_{\parallel} \cdot [\![\boldsymbol{D}_{\parallel}]\!] \tag{2}$$

$$[\![\boldsymbol{E}_{\parallel}]\!] = -d_{\perp}\nabla_{\parallel}[\![\boldsymbol{E}_{\perp}]\!] \tag{3}$$

$$[\![\boldsymbol{B}_{\perp}]\!] = 0 \tag{4}$$

where the operator [[ ]] means the difference across the interface for the quantity inside the bracket, i.e., $[\![D_z]\!] = D_z(0^+) - D_z(0^-)$. The

subscript "||" means parallel to the interface (in x or y directions), while "⊥" means perpendicular to the interface (in z-direction), $\mathbf{n}_{12}$ is the unit vector from medium 1 to medium 2, i.e., along the z-direction. The gradient operator $\nabla_{\parallel} = \left(\hat{x}\frac{\partial}{\partial x} + \hat{y}\frac{\partial}{\partial y}\right) = \hat{x}ik_x$. Through the derivation (see Methods), the Feibelman parameters $d_{\parallel}$ and $d_{\perp}$ naturally emerge

$$d_{\perp} = \frac{\int_{z_1}^{z_2} z\frac{dE_z}{dz}dz}{\int_{z_1}^{z_2}\frac{dE_z}{dz}dz} = \frac{\int_{z_1}^{z_2} z\rho(z)dz}{\int_{z_1}^{z_2}\rho(z)dz} = \boldsymbol{d}_{\perp}\cdot\boldsymbol{n}_{12} \tag{5a}$$

$$d_{\parallel} = \frac{\int_{z_1}^{z_2} z\frac{dD_x}{dz}dz}{\int_{z_1}^{z_2}\frac{dD_x}{dz}dz} = \frac{\int_{z_1}^{z_2} z\frac{\partial P_x}{\partial z}dz}{\int_{z_1}^{z_2}\frac{\partial P_x}{\partial z}dz} = \frac{\int_{z_1}^{z_2} z\frac{\partial J_x}{\partial z}dz}{\int_{z_1}^{z_2}\frac{\partial J_x}{\partial z}dz} = \boldsymbol{d}_{||}\cdot\boldsymbol{n}_{12} \tag{5b}$$

The real part of $d_{\perp}$ measures the spatial deviation of the induced surface charge from $z = 0$, i.e., the centroid of induced surface charge, and the real part of $d_{\parallel}$ is a measure of the location of the gradient of the induced polarization parallel to the surface, i.e., the Feibelman parameters are the surface response functions. The imaginary parts are related to dissipation, which we will discuss more later. In Eqs. (5a) and (5b), we have used vectors $\boldsymbol{d}_{\perp}$ and $\boldsymbol{d}_{\parallel}$ to emphasize that the Feibelman parameters depend on the choice of coordinate, in addition to the choice of surface norm direction $\mathbf{n}_{12}$. If the direction of the z-coordinate in Fig. 1b is flipped, the sign of the Feibelman parameters should be flipped too. This way, the spatial deviations as represented by the real parts of the Feibelman parameters remain unchanged.

The derivations we present (see Methods) do not depend on the substrate other than assuming it has an isotropic macroscopic dielectric constant. Schaich and Chen[31] had considered the anisotropy of the interfacial region and arrived at a 3×3 matrix for the d-parameters. However, their results also suggest that only $d_{\parallel}$ and $d_{\perp}$ as defined above are important when $d_{\parallel}$ is modified via a proper averaging invoking the azimuthal angle between the plane of incidence and the principal axes of the interface. Extensions to include anisotropy of the substrate as well as the anisotropy of the d-parameters might be needed for the case of anisotropic substrates.

The important implications of the generalized boundary conditions derivations are that (1) the interfacial region in any material is never sharp, and (2) the Feibelman parameters combined with generalized boundary conditions for the Maxwell equations can be used to include such interfacial regions. We can see that when the Feibelman parameters are zero, Eqs. (1–4) become the classical boundary conditions for the Maxwell equations. The Feibelman parameters represent the correction caused by the transition region at the interface. This is sketched in Fig. 1b. Rather than the discontinuity represented by the red lines in E_z from the classical boundary conditions, the rapid change over a finite thickness leads to a different value of E_z on the $z = 0^+$ side. Despite that E_z reaches the final value over a small distance, we approximate this as an abrupt change at the interface, i.e., the blue line extends back to the interface.

We should emphasize that the derivation (see Methods) does not give values of the Feibelman parameters, which can only be resolved by microscopic models, as have been done for electrons at metallic surfaces[14,15]. For now, such a microscopic model is still lacking for the photomolecular effect. Next, we will use these boundary conditions to explain some of the photomolecular experiments at a single water-air interface, treating the Feibelman parameters as adjustable parameters that can be determined based on experimental data.

Modified Fresnel coefficients and surface absorptance

Using the general boundary conditions (1–4), it is straightforward to derive new expressions for the interface reflection and transmission coefficients that differ from the Fresnel coefficients, which were derived based on the classical boundary conditions. Understandably, however, the deviations are small. Such expressions have been partially given in the literature[14,15,31,32,34]. Since these studies deal with absorbing substrates, i.e., mostly metals, the focus usually was on the reflection coefficient or reflectance that is directly measurable, with the exception of Goncalves et al.[34], who also give expression for transmittance. Our focus will be on the interface absorptance so that we can compare with experiments at an air-water interface[2]. For completeness, we will also give the interface reflectance and transmittance. In the Methods section, we show detailed derivations. For an incident TM-polarized wave, the reflection (r_p) and transmission (t_p) coefficients are given by

$$r_p = -\frac{\sqrt{\varepsilon_{r1}}\hat{k}_{z2} - \sqrt{\varepsilon_{r2}}\hat{k}_{z1} - (\varepsilon_{r1}-\varepsilon_{r2})ik_o\left(d_{\perp}\hat{k}_{x1}\hat{k}_{x2} - d_{||}\hat{k}_{z1}\hat{k}_{z2}\right)}{\sqrt{\varepsilon_{r1}}\hat{k}_{z2} + \sqrt{\varepsilon_{r2}}\hat{k}_{z1} - (\varepsilon_{r1}-\varepsilon_{r2})ik_o\left(d_{\perp}\hat{k}_{x1}\hat{k}_{x2} + d_{||}\hat{k}_{z1}\hat{k}_{z2}\right)} \tag{6}$$

$$t_p = \frac{2\sqrt{\varepsilon_{r1}}\hat{k}_{z1}}{\sqrt{\varepsilon_{r1}}\hat{k}_{z2} + \sqrt{\varepsilon_{r2}}\hat{k}_{z1} - (\varepsilon_{r1}-\varepsilon_{r2})ik_o\left(d_{\perp}\hat{k}_{x1}\hat{k}_{x2} + d_{||}\hat{k}_{z2}\hat{k}_{z1}\right)} \tag{7}$$

where $\varepsilon = \varepsilon_o\varepsilon_r$ is the electrical permittivity and ε_r the dielectric constant. The wavevector along the interface direction $k_{x1} = 2\pi N_1\sin\theta_1/\lambda_o = k_{x2} = 2\pi N_2\sin\theta_2/\lambda_o$ due to conservation of the lateral photon momentum, with the refractive index $N = \sqrt{\varepsilon_r}$, $k_{z1} = 2\pi N_1\cos\theta_1/\lambda_o$ and $k_{z2} = 2\pi N_2\cos\theta_2/\lambda_o$, $k_o = 2\pi/\lambda_o$ the magnitude of the free-space wavevector, and the unit vector $(\hat{k}_{x1}, 0, \hat{k}_{z1}) = (\sin\theta_1, 0, \cos\theta_1)$, $(\hat{k}_{x2}, 0, \hat{k}_{z2}) = (\sin\theta_2, 0, \cos\theta_2)$. If $d_{||} = 0$ and $d_{\perp} = 0$, the above equations reduce to the Fresnel reflection ($r_{p,F}$) and transmission ($t_{p,F}$) coefficients [see Methods, Eqs. (48) and (49)]. Using these coefficients and Taylor expansion, retaining only first order terms in the Feibelman parameters, we can further write Eqs. (6) and (7) as

$$r_p \approx r_{p,F}\left\{1 - \frac{2(\varepsilon_{r2}-\varepsilon_{r1})}{\varepsilon_{r1}\hat{k}_{z2}^{\,2} - \varepsilon_{r2}\hat{k}_{z1}^{\,2}}ik_{z1}\left[\hat{k}_{z2}^{\,2}d_{||} - \hat{k}_{x1}^{\,2}d_{\perp}\right]\right\} \tag{8}$$

$$t_p \approx t_{p,F}\left\{1 - \frac{(\varepsilon_{r2}-\varepsilon_{r1})ik_o\left(d_{\perp}\hat{k}_{x1}\hat{k}_{x2} + d_{||}\hat{k}_{z2}\hat{k}_{z1}\right)}{\sqrt{\varepsilon_{r1}}\hat{k}_{z2} + \sqrt{\varepsilon_{r2}}\hat{k}_{z1}}\right\} \tag{9}$$

From the reflection and transmission coefficients, the reflectance (R_p) and transmittance (τ_p) can be calculated from $R_p = |r_p|^2$ and $\tau_p = \left\{Re\left[N_2^*(\cos\theta_2)\right]/Re\left[N_1\cos\theta_1\right]\right\}|t_p|^2$, and the interface absorptance is $A_p = 1 - R_p - \tau_p$. When both ε_{r1} and ε_{r2} are real, the reflectance, transmittance, and absorptance expressed using the more-familiar angles of incidence and refraction (for other forms see Methods) are

$$R_p = R_{p,F}\left\{1 + \frac{4(n_2^2 - n_1^2)}{n_1^2\cos^2\theta_2 - n_2^2\cos^2\theta_1}\frac{2\pi n_1}{\lambda_o}\cos\theta_1\left[d_{||i}\cos^2\theta_2 - d_{\perp i}\sin^2\theta_1\right]\right\} \tag{10}$$

$$\tau_p = \tau_{p,F}\left\{1 + \frac{2(n_2^2 - n_1^2)}{n_1\cos\theta_2 + n_2\cos\theta_1}\frac{2\pi}{\lambda_o}\left(d_{\perp i}\sin\theta_1\sin\theta_2 + d_{||i}\cos\theta_1\cos\theta_2\right)\right\} \tag{11}$$

$$A_p = -\frac{4(n_2^2 - n_1^2)}{(n_1\cos\theta_2 + n_2\cos\theta_1)^2}\frac{2\pi n_1}{\lambda_o}\cos\theta_1\left(d_{||i}\cos^2\theta_2 + d_{\perp i}\sin^2\theta_1\right) \tag{12}$$

where n means that the refractive index N is real. The last expressions show two interesting points: (1) the reflectance, transmittance, and absorptance

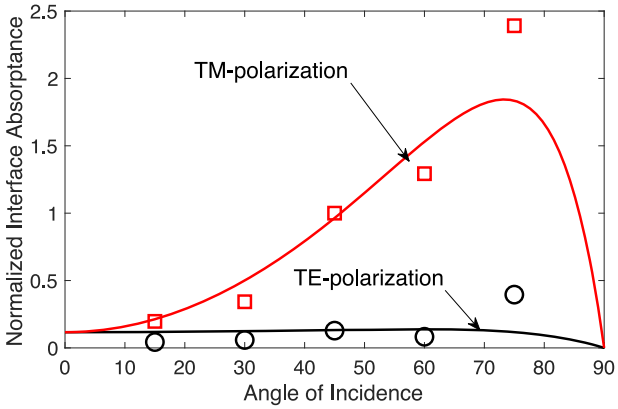

Fig. 2 | Comparison with experiments. Beam bending experimental data points for both TM and TE polarizations of a 520 nm laser were normalized by experimental value for the TM-polarization at 45°. Theoretical interface absorptance values calculated from Eqs. (12) and (18) were also normalized to the calculated value for TM polarization at 45°. Best fitted value for $d_{||i}/d_{\perp i}$ is 0.08.

only depend on the imaginary parts of the Feibelman parameters and (2) the imaginary parts of the Feibelman parameters should be negative when $\varepsilon_{r1} < \varepsilon_{r2}$ so that the absorptance is positive. Equation (12) is consistent with the absorbed power at the interface [see Eq. (73), Methods]:

$$P_p(\omega) = -\frac{\omega}{2}\varepsilon_o(\varepsilon_{r2}-\varepsilon_{r1})\frac{4\varepsilon_1\varepsilon_2 k_{z1}k_{z1}^*}{\left[\varepsilon_1 k_{z1}+\varepsilon_2 k_{z2}\right]^2}|E_i|^2\left[cos^2\theta_2\, d_{||i}+sin^2\theta_1 d_{\perp i}\right] \tag{13}$$

Dividing the above expression by the incident power per unit area of the interface, i.e., the z-component of the Poynting vector $S_{p,z} = \mathrm{Re}(E_{ix}H_{iy}^*)/2 = k_{z1}|E_i|^2/(2\mu\omega)$, leads to Eq. (12).

Note that Eqs. (12) and (13) mean that if light is incident from the high refractive index side, the imaginary parts should become positive. This is taken care by going back to the vector representation of the Feibelman parameters as expressed in Eqs. (5a) and (5b).

For the TE-polarization, the reflection and transmission coefficients are

$$\begin{aligned} r_s &= \frac{\sqrt{\varepsilon_{r1}}\hat{k}_{z1}-\sqrt{\varepsilon_{r2}}\hat{k}_{z2}-ik_o d_{||}(\varepsilon_{r2}-\varepsilon_{r1})}{\sqrt{\varepsilon_{r1}}\hat{k}_{z1}+\sqrt{\varepsilon_{r2}}\hat{k}_{z2}+ik_o d_{||}(\varepsilon_{r2}-\varepsilon_{r1})} \\ &\approx r_{s,F}\left[1-\frac{2ik_{z1}d_{||}(\varepsilon_{r2}-\varepsilon_{r1})}{\left(\sqrt{\varepsilon_{r1}}\hat{k}_{z1}\right)^2-\left(\sqrt{\varepsilon_{r2}}\hat{k}_{z2}\right)^2}\right] \end{aligned} \tag{14}$$

$$\begin{aligned} t_s &= \frac{2\sqrt{\varepsilon_{r1}}\hat{k}_{z1}}{\sqrt{\varepsilon_{r1}}\hat{k}_{z1}+\sqrt{\varepsilon_{r2}}\hat{k}_{z2}+ik_o d_{||}(\varepsilon_{r2}-\varepsilon_{r1})} \\ &\approx t_{s,F}\left[1-\frac{ik_o d_{||}(\varepsilon_{r2}-\varepsilon_{r1})}{\sqrt{\varepsilon_{r1}}\hat{k}_{z1}+\sqrt{\varepsilon_{r2}}\hat{k}_{z2}}\right] \end{aligned} \tag{15}$$

with $r_{s,F}$ and $t_{s,F}$ the Fresnel coefficients for the TE-polarization [see Method, Eqs. (65) and (66)]. For real ε_{r1} and ε_{r2}, the corresponding reflectance, transmittance, and absorptance are

$$R_s = R_{s,F}\left(1+\frac{4(n_2^2-n_1^2)}{n_1^2\cos^2\theta_1-n_2^2\cos^2\theta_2}\frac{2\pi n_1}{\lambda_o}\cos\theta_1 d_{||i}\right) \tag{16}$$

$$\tau_s = \tau_{s,F}\left(1+\frac{2(n_2^2-n_1^2)}{n_1\cos\theta_1+n_2\cos\theta_2}\frac{2\pi}{\lambda_o}\mathrm{d}_{||i}\right) \tag{17}$$

$$A_s \approx \frac{-4(n_2^2-n_1^2)}{\left[n_1\cos\theta_1+n_2\cos\theta_2\right]^2}\frac{2\pi n_1}{\lambda_o}\cos\theta_1 \mathrm{d}_{||i} \tag{18}$$

One can follow similar procedure to show that this interface absorptance expression is consistent with the expression for the absorbed power for the TE polarization [see Eq. (74), Methods]. This expression again shows that the imaginary part of Feibelman parameter $d_{||i}$ is negative when $\varepsilon_{r1} < \varepsilon_{r2}$ and changes sign when light enters from medium 2. Equation (18) shows that there is absorption even for TE-polarization. Conceptually, when a dipole orientation differs from the $\theta = 0°$, the dipole could be set into motion by both x and z-directions by the TM-polarized light, which explains why both $d_{\perp i}$ and $\mathrm{d}_{||i}$ appeared in Eq. (12). For TE-polarized light, the motion is in the x-direction, which explains why only $\mathrm{d}_{||i}$ appears in Eq. (18).

We can further appreciate why the imaginary part $d_{||i}$ must be negative as follows. The energy dissipated by an electromagnetic wave can be expressed as $\boldsymbol{Re}[\boldsymbol{J}(z)\cdot\boldsymbol{E}^*(z)]/2$. If there is no additional phase lag between **E** and **P**, i.e., the electric susceptibility χ is real, there is no dissipation since $\mathbf{J}=-i\omega\boldsymbol{P}(\omega,\boldsymbol{r}) = -i\omega\varepsilon_o\chi\boldsymbol{E}(\omega,\boldsymbol{r})$ (see Methods). In this case, the current lags behind the electrical field by 90°. Inside a homogeneous medium, the fact that the dissipated power $\boldsymbol{Re}[\boldsymbol{J}(z)\cdot\boldsymbol{E}^*(z)]/2$ should be positive means that Im(χ) must be positive. However, at an interface, the classical boundary conditions for the Maxwell equations lead to a surface current $\boldsymbol{J}_s = \boldsymbol{n}\times[\![\boldsymbol{H}]\!]$, using Eq. (1), we have $\boldsymbol{J}_s = i\omega d_{||}[\![\boldsymbol{D}_{//}]\!] \approx i\omega d_{||}\varepsilon_o(\varepsilon_{r2}-\varepsilon_{r1})\,\boldsymbol{E}_x$. Thus, when $\varepsilon_{r2} > \varepsilon_{r1}$, $d_{||i}$ must be negative if light comes from side 1.

Comparison with experiments

We now attempt to compare the above theory with some of the experimental results we had at a single air-water interface[2]. Before such comparison, we should clarify that accurate measurements of the interfacial absorptance remain a challenge. In the photomolecular evaporation experiments at a single air-water interface[2], we measured the slope of the change in the refraction angle with diode laser intensity, i.e., slope of the bending of the refracted beam, as a function of the incident angle and the polarization for lasers with the following wavelengths: 450 nm, 520 nm, 635 nm, and 850 nm. For all wavelengths, we observed much stronger responses for the TM polarization than the TE one. For the TM polarization, the beam bending shows strong dependence on the angle of incidence, peaking at 45° except for the 850 nm, which reaches a maximum at 60°. We determined that the beam bending was due to the air-side refractive index change caused by the water clusters cleaved into the air. However, we do not know if the beam bending dependence on wavelength was due to the absorptance or the cluster size dependence on the wavelength. For each wavelength, we can reasonably assume that the cluster size is fixed and hence the measured beam bending is proportional to the absorptance. We hence normalize the beam-bending experimental values at different angles to the beam-bending value of TM polarization at 45°, and fit the normalized values to the absorptance expressions, i.e., Eqs. (12) and (18), also normalized to the calculated value at 45° for the TM polarization, with $d_{||i}/d_{\perp i}$ as the fitting parameter. To convert the beam bending data point to absorptance, we divide each measured values by $\cos\theta_1$ because the beam bending is proportional to absorbed power, i.e., Eq. (13), which is related to the absorptance by $\cos\theta_1$.

Figure 2 shows a comparison of the theoretical values of normalized interface absorptance for 520 nm laser vs. angle of incidence against normalized experimental values of the beam bending. Similar curves can be plotted for other wavelengths. We see that although the beam-bending, which corresponds to evaporation, peaking around 45°, the absorptance is maximum around 75°. The angular dependence trends compare reasonably between experiment and theory. The fact that we can use the angle-independent Feibelman parameters to capture the angle dependence of the experimental data supports our interpretation of the photomolecular effect. The fitted $d_{||i}/d_{\perp i}$ value of 0.08 shows that $d_{\perp i}$ is much larger than $\mathrm{d}_{||i}$ for water, consistent with our picture that it is the rapidly changing electrical

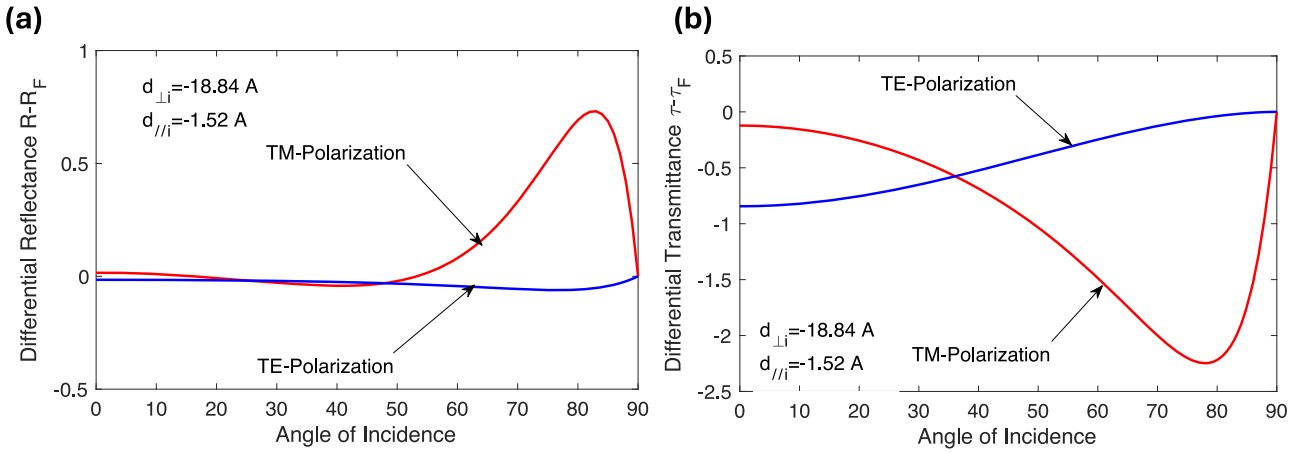

Fig. 3 | Differential reflectance and transmittance. Differences in (**a**) reflectance and (**b**) transmittance from the Fresnel values due to photomolecular effect at the interface, using imaginary parts of the Feibelman parameters obtained for 520 nm.

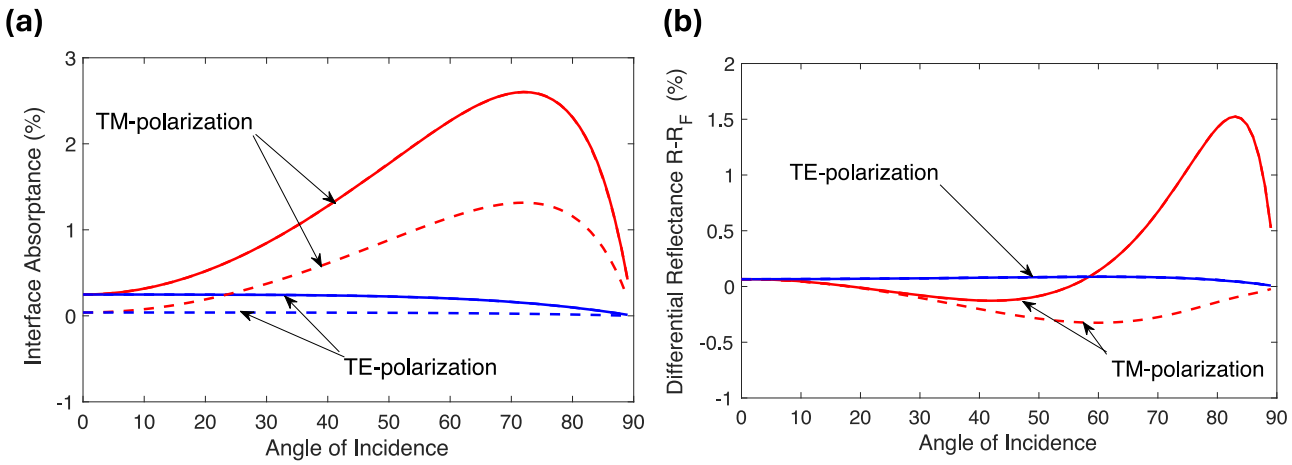

Fig. 4 | Impact of real parts of Feibelman parameters on absorption. a Interface absorptance and (**b**) differential reflectance when the bulk substrate is also absorbing, showing that they depend also on the real parts of the Feibelman parameters in such cases. Solid lines for $d_\perp = (-10^{-9}, -10^{-9})$ and $d_\parallel = (-10^{-10}, -10^{-10})$, dashed lines for $d_\perp = (10^{-9}, -10^{-9})$ and $d_\parallel = (10^{-10}, -10^{-10})$, $n_1 = 1$, and $N_2 = (1.5, 0.5)$.

field in the z-direction at the interface that is the main driving force for the photomoleuclar effect.

The actual values of $d_{\perp i}$ and $d_{||i}$ depend on the value of absorptance. Based on the measured temperature difference of water with and without the laser irradiation, we had inferred $A_p = 0.84\%$ for a TM-polarized green ($\lambda = 532$ nm) laser at 45° incident angle, assuming the same convection heat transfer coefficient applies. Applying the same absorptance value for $\lambda = 520$ nm, we get $d_{\perp i} \sim 18.8$ Å and $d_{||i} \sim 1.52$ Å. We cannot infer the real part of the Feibelman parameters from the absorptance values. In the past, the imaginary part of the Feibelman parameters computed for metal surfaces is a few Å[14,15]. The values we inferred for water are larger by a few times. Given the uncertainties in the absorptance and lack of detailed microscopic picture, we will refrain from further commenting on the reasonableness of the values.

Discussion

To see the impact of the Feibelman parameters on the reflectance and transmittance, we show in Fig. 3 the calculated differences in the reflectance and transmittance from the Fresnel formula, assuming bulk water does not absorb. While the transmittance becomes smaller due to the surface absorption for both TM- and TE-polarizations, the reflectance for the TE-polarization is smaller but the TM-polarization becomes larger at large angle of incidence.

When the substrate is also absorbing, we can no longer use the reflectance, transmittance and absorptance expressions given before. Instead, we need to use Eqs. (8) and (9) for TM-polarized light and Eqs. (14) and (15) for TE-polarized light to calculate reflectance and transmittance. We then obtain absorptance from $A = 1\text{-}R\text{-}\tau$. Figure 4 shows that the interface absorptance and reflectance will depend on both the real and the imaginary parts of the Feibelman parameters. One can think in this case, the real part of the Feibelman parameter creates some phase delay, which impacts the absorptance of the interfacial region and the coupling to the substrate, as often seen for a film on a substrate.

The above results showed that the generalized boundary conditions built on the Feibelman parameters can reasonably capture the angular and polarization dependence experimental data on an air-water interface, despite that these results were intended for metal surfaces. The reported angle and polarization dependence of the beam deflection experiments, when mapped onto absorptance, are in qualitative agreement with the modeling. Such agreements lend confidence to both the modeling approach and the photomolecular effect: photons are absorbed at air-water interface, leading to cleavage of water molecular clusters.

Our rederivation of the generalized boundary conditions for the Maxwell equations only assumes that the electrical and magnetic fields across an interface are continuous rather than discontinuous as typically used, independent of materials. The derivations naturally lead to the

Feibelman parameters derived originally to describe the response of metallic surfaces to electromagnetic fields. Hence, the Feibelman parameters are universal, rather than specific to metals. In the case of metals, the real part of $d_\perp(\lambda)$ represents the centroid location of the electrons while that of $d_{||}(\lambda)$ the location of the surface current. For nonmetals such as water, there are no free electrons. However, the nonuniform field at the interface creates an equivalent polarization charge[35]. To see this, we can take a dipole along z-direction at the interface and consider an electrostatic field (extension to eletrodynamic field using vector potential will lead to similar conclusion). The force acting on the dipole is $F = -qE_z(z) + E_z(z+h) = q\frac{dE}{dz}h$, where h is the separation between the charges. This force can be thought as arising from quadruple potential[8]. In a bulk material, $\frac{dE}{dz}$ is nearly zero and hence the quadruple term is not important. At the interface, however, $\frac{dE}{dz}h \sim f\left(E_{z2} - E_{z1}\right)$ with the factor f depending on the value of h and the electrical field gradient, leading to a quadruple force on the dipole, $F \sim fqE_{z1}$, which can be comparable to that on a free charge. For materials with permanent dipoles, such as water, f can be close to 1. Even for neutral atoms, h can still be non-zero due to induced dipole. Hence, the polarization charge created at the interface can be compared to electrons in metals, leading to nonzero Feibelman parameter values.

The imaginary parts of the Feibelman parameters represent dissipation. In metals, the dissipation can happen since the electrons at the surface can interact with the bulk electrons in the metal, or be excited to the free space via photoemission. In water, the displaced electrons at interface can dissipate their energy via interaction with ions and the hydrogen network, although the detailed mechanisms remain unclear. In nonmetallic solids, the excited polarization charge can dissipate their energy by interaction with phonons in the bulk. Hence, interfacial absorption should exist in many materials, which can be described using the Feibelman parameters.

The generalized boundary conditions enable one to assess the impacts of the interface absorption for different geometries via solving the Maxwell equations. Using the generalized boundary conditions for the Maxwell equations, we gave here complete expressions for the reflectance, transmittance, and surface absorptance. For nonabsorbing substrates, the reflectance, transmittance, and surface absorptance depend on the imaginary parts of the Feibelman parameters only. The sign of the imaginary parts depends on the magnitude of the dielectric constants. When the dielectric constant of the substrate is larger than that of the incoming medium, the imaginary parts of the Feibelman parameters must be negative. Although our paper dealt with a flat interface only, using the generalized boundary conditions and the Feibelman parameters, one should be able to re-examine a wide range of problems based on solving Maxwell equations, such as cloud absorption.

Methods

Derivation of generalized boundary conditions

Different authors have given derivations of the generalized boundary conditions for the Maxwell equations[14,31–34]. The derivations below are slightly different, emphasizing that the derivation is independent of materials across the interface. We start from the macroscopic Maxwell equations

$$\nabla \times \boldsymbol{E} = -\frac{\partial \boldsymbol{B}}{\partial t} \tag{19}$$

$$\nabla \times \boldsymbol{H} = \frac{\partial \boldsymbol{D}}{\partial t} \tag{20}$$

$$\nabla \cdot \boldsymbol{D} = 0 \tag{21}$$

$$\nabla \cdot \boldsymbol{B} = 0 \tag{22}$$

Here we assume no net free charge nor current on the surface. To establish the boundary conditions, we take a spill-box to cover both sides of an interface, as shown in Fig. 1b. In the derivation of traditional boundary conditions for the Maxwell equations, one takes the limit of zero thickness of the spill-box and assumes that the field on each side does not change when it approaches zero thickness[8,9]. This treatment, for example, leads to the continuity of the displacement field in the z-direction, but a discontinuity in the electrical field, as represented by two red bars in Fig. 1b. In reality, however, the electrical field varies continuously but rapidly over the thin interfacial region (black line in Fig. 1b). Details on how the field changes with z depend on microscopic models. Our goal is to take into account of such a rapid change by modifying the boundary conditions of the Maxwell equations, which will relate the macroscopic electrical and magnetic fields on the two sides of the interface $z = 0^+$ and $z = 0^-$. These fields may differ from given by the traditional boundary conditions, as indicated by the blue line in Fig. 1b.

TM-Wave. Let us consider a TM wave first. Equation (21) can be written as

$$\frac{\partial D_x}{\partial x} + \frac{\partial D_z}{\partial z} = 0 \tag{23}$$

The field has periodic variations in the x-direction, i.e., $\boldsymbol{D} = \left(D_x(z)e^{ik_x x}, 0, D_z(z)\right)e^{-i\omega t}$, Eq. (23) can be written as

$$ik_x D_x(z) + \frac{dD_z}{dz} = 0 \tag{24}$$

Integrating the above equation, we have

$$D_z(z_2) - D_z(z_1) = -ik_x\left\{\left[z_2 D_x(z_2) - z_1 D_x(z_1)\right] - \int_{z_1}^{z_2} z\frac{dD_x}{dz}dz\right\} \tag{25}$$

Define

$$d_{||} = \frac{\int_{z_1}^{z_2} z\frac{dD_x}{dz}dz}{\int_{z_1}^{z_2}\frac{dD_x}{dz}dz} = \boldsymbol{d}_{||}\cdot\boldsymbol{n_{12}} \tag{26}$$

where again the vector $\boldsymbol{d}_{||}$ emphasizes that $d_{||}$ is measured along $\mathbf{n}_{12}$ direction. The integral on the numerator is a small but a finite value if we extend z_1 and z_2 to infinity, because only regions where D_x changes rapidly matter in the integration. $\boldsymbol{d}_{||}$ thus can be considered as a surface property. The goal of boundary condition is to establish relationship of the fields on the two sides of the interface. For such a purpose, we set the limits of z_1 and z_2 to 0^- and 0^+, Eq. (25) becomes

$$D_z(0^+) - D_z(0^-) = ik_x d_{||}\left[D_x(0^+) - D_x(0^-)\right] \tag{27}$$

This condition differs from the classical $D_z(0^+) - D_z(0^-) = 0$. The deviation is caused by the finite region when D_x changes from one side to the other, which is represented by $d_{||}$.

From Eqs. (19) and (20), eliminating **B** and **H** leads to

$$\nabla(\nabla\cdot\boldsymbol{E}) - \nabla^2\boldsymbol{E} = \mu\omega^2\boldsymbol{D} = \mu_o c_o^2 k_o^2 \boldsymbol{D} \tag{28}$$

where we assume no magnetic response, and subscript "o" represents vacuum, μ_o, c_o, and k_o the magnetic permeability, speed of light, and magnitude of the wavevector.

Next, we consider that variations in the x-direction, i.e., parallel to interface, can all be expressed as $e^{ik_x x}$, for example, $E_z(x,z) = E_z(z)\ e^{ik_x x}$, $E_x(x,z) = E_x(z)e^{ik_x x}$, $D_x(x,z) = D_x(z)e^{ik_x x}$. The x and z components of Eq. (28) are

$$ik_x\frac{dE_z}{dz} - \frac{d^2E_x}{dz^2} = \mu_o c_o^2 k_o^2 D_x \tag{29}$$

$$ik_x\frac{dE_x}{dz}+k_x^2E_z=\mu_o c_o^2k_o^2D_z \tag{30}$$

Taking derivative of both sides of Eq. (30), d/dz, and combining with Eq. (29) lead to Eq. (24). Hence Eq. (29) is redundant. Integrating Eq. (30) leads to

$$\begin{aligned}E_x(z_2)=&E_x(z_1)+\frac{\mu_o c_o^2k_o^2}{ik_x}\int_{z_1}^{z_2}D_z(z')dz'\\&+ik_x\left\{z_2E_z(z_2)-z_1E_z(z_1)-\int_{z_1}^{z_2}z'\frac{dE_z(z')}{dz'}dz'\right\}\end{aligned} \tag{31}$$

Since D_z does not change much based on the classical boundary conditions, the second term is negligible in the limit of z_1 and z_2 approaching 0. The above equation can be written as

$$E_x(0^+)-E_x(0^-)=-ik_xd_\perp\left(E_z(0^+)-E_z(0^-)\right) \tag{32}$$

where

$$d_\perp=\frac{\int_{z_1}^{z_2}z\frac{dE_z}{dz}dz}{\int_{z_1}^{z_2}\frac{dE_z}{dz}dz}=\boldsymbol{d}_\perp\cdot\boldsymbol{n_{12}} \tag{33}$$

Now, we consider the magnetic field $\boldsymbol{H}=(0,H_y(z)e^{ik_xx},0)e^{-i\omega t}$ for the TM wave, Eq. (22) is automatically satisfied. Equation (20) leads to

$$\frac{dH_y}{dz}=i\omega D_z(z) \tag{34}$$

Integrate the above equation and take the same limits as before, we arrive at

$$H_y(0^+)-H_y(0^-)=-i\omega d_{||}\left[D_x(0^+)-D_x(0^-)\right] \tag{35}$$

TE-Wave. For a TE wave with the $(0,\ E_y(z)e^{ik_xx},0)e^{-i\omega t}$, Eq. (21) is always satisfied. From Eqs. (19) and (20), we have

$$-\frac{dE_y}{dz}=\mu i\omega H_x(z) \tag{36}$$

$$\left[ik_x^2E_y-\mu\omega\frac{dH_x}{dz}\right]=i\mu\omega^2D_y(z) \tag{37}$$

Integrating Eq. (36) and invoking that H_x changes little over the interface per classical boundary condition, we have

$$E_y(0^+)-E_y(0^-)=0 \tag{38}$$

Integrating Eq. (37), we get

$$H_x(0^+)-H_x(0^-)=i\omega d_{||}\left[D_y(0^+)-D_y(0^-)\right] \tag{39}$$

One could also apply the same procedure to Eq. (22) to show that $B_z(0^+)-B_z(0^-)=0$.

The above interfacial conditions, i.e., Eqs. (27), (32), (35), (38), and (39), can be cast compactly as Eqs. (1–4)[32]. We note that both Eqs. (32) and (38) are represented by Eq. (3) since for TE-polarization, $\boldsymbol{E}_\perp$ is zero. Equation (2) leads to Eq. (35) when applied to a TM wave, and to Eq. (39) for a TE wave.

Feibelman parameters. The above derivation suggests that the Feibelman parameters defined in Eqs. (26) and (33) can be functions of frequency but not the in-plane wavevectors, i.e., they are independent of the angle of incidence. Their physical meaning can be better appreciated by connecting displacement to the charge and current via the constitutive relation, $\boldsymbol{D}=\varepsilon_o\boldsymbol{E}+\boldsymbol{P}$, where $\mathbf{P}$ is the electrical polarization. Gauss' law then leads to

$$\varepsilon_o\nabla\boldsymbol{E}=-\nabla\cdot\boldsymbol{P} \tag{40}$$

which also means that the induced charge, or the polarization charge, ρ

$$\nabla\cdot\boldsymbol{P}=-\rho \tag{41}$$

If we further define

$$\frac{\partial\boldsymbol{P}}{\partial t}=\boldsymbol{J} \tag{42}$$

So that we can write Eq. (3) as

$$\nabla\times\boldsymbol{H}=\varepsilon_o\frac{\partial\boldsymbol{E}}{\partial t}+\boldsymbol{J} \tag{43}$$

Such definitions satisfy the continuity relation

$$\frac{\partial\boldsymbol{\rho}}{\partial t}+\nabla\cdot\boldsymbol{J}=\mathbf{0} \tag{44}$$

Equations (40) and (43) resemble the microscopic Maxwell equation (although $\mathbf{E}$ and $\mathbf{H}$ are defined macroscopically). Thus, ρ and $\mathbf{J}$ can be understood as the microscopic charge density and polarization, related to polarization density $\mathbf{P}$. If we write $\mathbf{E}$ and ρ all in Fourier component $(E_x(z)e^{ik_xx},0,E_z(z)e^{ik_xx})$, ρe^{ik_xx}, Eqs. (40) and (41) lead to

$$ik_xE_x+\frac{dE_z}{dz}=\frac{\rho}{\varepsilon_o} \tag{45}$$

The first term on the left hand side of Eq. (45) is much smaller than the second term and hence can be neglected (i.e., the so-called DC limit $k_x=0$). Thus, the Feibelman parameters can also be written in different forms as expressed by Eq. (5).

Reflectance, transmittance, and absorptance

Different authors have given expressions for the interface reflection coefficients, and in some cases, the transmission coefficients too[14,15,31,34]. However, none of them give complete expressions for reflectance, transmittance, and especially interface absorptance. In the following, we will give complete expressions for both TM and TE polarizations. Details of the derivation are given in the Supplementary Methods.

TM-Wave. The Fresnel reflection (r_p) and transmission (t_p) coefficients for a TM-polarized incident wave as shown in Fig. 1c are,

$$r_p=\frac{-\frac{\varepsilon_1\hat{k}_{x1}+d_{||}ik_{x1}\varepsilon_1\hat{k}_{z1}}{(\varepsilon_2\hat{k}_{x2}+d_{||}ik_{x1}\varepsilon_2\hat{k}_{z2})}+\frac{\hat{k}_{z1}-d_\perp ik_{x1}\hat{k}_{x1}}{(\hat{k}_{z2}-d_\perp ik_{x1}\hat{k}_{x2})}}{\frac{(\varepsilon_1\hat{k}_{x1}-d_{||}ik_{x1}\varepsilon_1\hat{k}_{z1})}{(\varepsilon_2\hat{k}_{x2}+d_{||}ik_{x1}\varepsilon_2\hat{k}_{z2})}+\frac{(\hat{k}_{z1}+d_\perp ik_{x1}\hat{k}_{x1})}{(\hat{k}_{z2}-d_\perp ik_{x1}\hat{k}_{x2})}} \tag{46}$$

$$t_p=\frac{\frac{\varepsilon_1\hat{k}_{x1}+d_{||}ik_{x1}\varepsilon_1\hat{k}_{z1}}{(\varepsilon_1\hat{k}_{x1}-d_{||}ik_{x1}\varepsilon_1\hat{k}_{z1})}+\frac{\hat{k}_{z1}-d_\perp ik_{x1}\hat{k}_{x1}}{(\hat{k}_{z1}+d_\perp ik_{x1}\hat{k}_{x1})}}{\frac{(\varepsilon_2\hat{k}_{x2}+d_{||}ik_{x1}\varepsilon_2\hat{k}_{z2})}{(\varepsilon_1\hat{k}_{x1}-d_{||}ik_{x1}\varepsilon_1\hat{k}_{z1})}+\frac{(\hat{k}_{z2}-d_\perp ik_{x1}\hat{k}_{x2})}{(\hat{k}_{z1}+d_\perp ik_{x1}\hat{k}_{x1})}} \tag{47}$$

If $d_{||}=0$ and $d_\perp=0$, the above equations reduce to the Fresnel coefficients

$$\begin{aligned}r_{p,F}&=-\frac{\varepsilon_1\hat{k}_{x1}\hat{k}_{z2}-\varepsilon_2\hat{k}_{x2}\hat{k}_{z1}}{\varepsilon_1\hat{k}_{x1}\hat{k}_{z2}+\varepsilon_2\hat{k}_{x2}\hat{k}_{z1}}=\frac{\sqrt{\varepsilon_{r1}}k_{2z}-\sqrt{\varepsilon_{r2}}k_{1z}}{\sqrt{\varepsilon_{r1}}k_{2z}+\sqrt{\varepsilon_{r2}}k_{1z}}\\&=-\frac{N_1cos\theta_2-N_2cos\theta_1}{N_1cos\theta_2+N_2cos\theta_1}\end{aligned} \tag{48}$$

$$t_{p,F} = \frac{2\varepsilon_1 \hat{k}_{x1}\hat{k}_{z1}}{\varepsilon_2 \hat{k}_{x2}\hat{k}_{z1} + \varepsilon_1 \hat{k}_{x1}\hat{k}_{z2}} = \frac{2\sqrt{\varepsilon_{r1}}\hat{k}_{z1}}{\sqrt{\varepsilon_{r1}}\hat{k}_{z2} + \sqrt{\varepsilon_{r2}}\hat{k}_{z1}} = \frac{2N_1 cos\theta_1}{N_1 cos\theta_2 + N_2 cos\theta_1} \tag{49}$$

By retaining only the first order terms in the Feibelman parameters, we can simplify Eq. (46) as

$$\begin{aligned} r_p &\approx -\frac{\varepsilon_1 \hat{k}_{x1}\hat{k}_{z2} - \varepsilon_2 \hat{k}_{x2}\hat{k}_{z1} - (\varepsilon_1 - \varepsilon_2) ik_{x1}\left(d_\perp \hat{k}_{x1}\hat{k}_{x2} - d_{||}\hat{k}_{z1}\hat{k}_{z2}\right)}{\varepsilon_1 \hat{k}_{x1}\hat{k}_{z2} + \varepsilon_2 \hat{k}_{x2}\hat{k}_{z1} - (\varepsilon_1 - \varepsilon_2) ik_{x1}\left(d_\perp \hat{k}_{x1}\hat{k}_{x2} + d_{||}\hat{k}_{z1}\hat{k}_{z2}\right)} \\ &= -\frac{\sqrt{\varepsilon_{r1}}\hat{k}_{z2} - \sqrt{\varepsilon_{r2}}\hat{k}_{z1} - (\varepsilon_{r1} - \varepsilon_{r2}) ik_o\left(d_\perp \hat{k}_{x1}\hat{k}_{x2} - d_{||}\hat{k}_{z1}\hat{k}_{z2}\right)}{\sqrt{\varepsilon_{r1}}\hat{k}_{z2} + \sqrt{\varepsilon_{r2}}\hat{k}_{z1} - (\varepsilon_{r1} - \varepsilon_{r2}) ik_o\left(d_\perp \hat{k}_{x1}\hat{k}_{x2} + d_{||}\hat{k}_{z1}\hat{k}_{z2}\right)} \end{aligned} \tag{51}$$

The above can also be written into a form identical to that of Eq. (S13) in Ref. 32

$$r_p = -\frac{\varepsilon_1 k_{2z} - \varepsilon_2 k_{1z} - i(\varepsilon_1 - \varepsilon_2)\left(d_\perp k_{x1}^2 - d_{||}k_{z1}k_{z2}\right)}{\varepsilon_1 k_{2z} + \varepsilon_2 k_{1z} - i(\varepsilon_1 - \varepsilon_2)\left(d_\perp k_{x1}^2 + d_{||}k_{z1}k_{z2}\right)} \tag{52}$$

We can further approximate Eq. (52) as

$$\begin{aligned} r_p &= r_{p,F}\left\{1 - \frac{2(\varepsilon_{r2} - \varepsilon_{r1}) ik_{z1}}{\varepsilon_{r1}\hat{k}_{z2}^{\ 2} - \varepsilon_{r2}\hat{k}_{z1}^{\ 2}}\left[\hat{k}_{z2}^2 d_{||} - \hat{k}_{x1}^2 d_\perp\right]\right\} \\ &= r_{p,F}\left\{1 - \frac{2\left(\frac{\varepsilon_2}{\varepsilon_1} - 1\right) ik_{z1}}{k_{z2}^2 - \left(\frac{\varepsilon_2}{\varepsilon_1}\right)^2 k_{z1}^2}\left[k_{z2}^2 d_{||} - \frac{\varepsilon_2}{\varepsilon_1}k_{x1}^2 d_\perp\right]\right\} \end{aligned} \tag{53}$$

The last expression is identical to Feibelman's Eq. (2.81)[14].

Next, we examine the transmission coefficient, Eq. (47), which can be approximated as

$$\begin{aligned} t_p &\approx \frac{2\varepsilon_{r1}\hat{k}_{x1}\hat{k}_{z1}}{\varepsilon_{r2}\hat{k}_{x2}\hat{k}_{z1} + \varepsilon_1 \hat{k}_{x1}\hat{k}_{z2} + (\varepsilon_{r2} - \varepsilon_{r1}) ik_{x1}\left(d_\perp \hat{k}_{x1}\hat{k}_{x2} + d_{||}\hat{k}_{z2}\hat{k}_{z1}\right)} \\ &\approx t_{p,F}\left\{1 - \frac{(\varepsilon_{r2} - \varepsilon_{r1}) ik_o\left(d_\perp \hat{k}_{x1}\hat{k}_{x2} + d_{||}\hat{k}_{z2}\hat{k}_{z1}\right)}{\sqrt{\varepsilon_{r2}}\hat{k}_{z1} + \sqrt{\varepsilon_{r1}}\hat{k}_{z2}}\right\} \end{aligned} \tag{54}$$

Typically, ε_{r1} is real and ε_{r2} is complex. The Poynting vector normal to the interface is

$$S_{z,i} = \frac{E_i E_i^*}{2\mu c_o} Re\left(\hat{k}_z N^*\right) \tag{55}$$

We can calculate the reflectance and transmittance from

$$R_p = |r_p|^2 \text{and } \tau_p = \frac{Re\left[\hat{k}_{z2}N_2^*\right]}{k_{z1}}|t_p|^2 = \frac{Re\left[N_2{}^* cos\theta_2\right]}{Re\left[n_1 cos\theta_1\right]}|t_p|^2 \tag{56}$$

And the absorptance is then

$$A_p = 1 - R_p - \tau_p \tag{57}$$

where we assume $N_1 = n_1 = \sqrt{\varepsilon_{r1}}$ is real, since when N_1 is complex, there will be absorption at the interface[36], which will further complicate the discussion. When ε_{r2} is complex, there will be coupling between the absorption in the substrate and the interface. However, when both ε_{r1} and ε_{r2} are real, i.e., no absorption in the bulk material, we can write the reflection and transmission coefficients using the real and imaginary parts of the Feibelman parameters $d_\perp = d_{\perp r} + id_{\perp i}$ and $d_{||} = d_{||r} + id_{||i}$ as

$$r_p = -\frac{\sqrt{\varepsilon_{r1}}\hat{k}_{z2} - \sqrt{\varepsilon_{r2}}\hat{k}_{z1} + (\varepsilon_{r1} - \varepsilon_{r2})k_o\left(d_{\perp i}\hat{k}_{x1}\hat{k}_{x2} - d_{||i}\hat{k}_{z1}\hat{k}_{z2}\right) - (\varepsilon_{r1} - \varepsilon_{r2})ik_o\left(d_{\perp r}\hat{k}_{x1}\hat{k}_{x2} - d_{||r}\hat{k}_{z1}\hat{k}_{z2}\right)}{\sqrt{\varepsilon_{r1}}\hat{k}_{z2} + \sqrt{\varepsilon_{r2}}\hat{k}_{z1} + (\varepsilon_{r1} - \varepsilon_{r2})k_o\left(d_{\perp i}\hat{k}_{x1}\hat{k}_{x2} + d_{||i}\hat{k}_{z1}\hat{k}_{z2}\right) - (\varepsilon_{r1} - \varepsilon_{r2})ik_o\left(d_{\perp r}\hat{k}_{x1}\hat{k}_{x2} + d_{||r}\hat{k}_{z1}\hat{k}_{z2}\right)} \tag{58}$$

$$t_p = \frac{2\sqrt{\varepsilon_{r1}}\hat{k}_{z1}}{\sqrt{\varepsilon_{r1}}\hat{k}_{z2} + \sqrt{\varepsilon_{r2}}\hat{k}_{z1} + (\varepsilon_{r1} - \varepsilon_{r2})k_o\left(d_{\perp i}\hat{k}_{x1}\hat{k}_{x2} + d_{||i}\hat{k}_{z2}\hat{k}_{z1}\right) - (\varepsilon_{r1} - \varepsilon_{r2})ik_o\left(d_{\perp r}\hat{k}_{x1}\hat{k}_{x2} + d_{||r}\hat{k}_{z2}\hat{k}_{z1}\right)} \tag{59}$$

From which we get (keeping only up to first order in the d-parameters)

$$\begin{aligned} R_p &\approx \frac{\left[\sqrt{\varepsilon_{r1}}\hat{k}_{z2} - \sqrt{\varepsilon_{r2}}\hat{k}_{z1}\right]^2 + 2\left(\sqrt{\varepsilon_{r1}}\hat{k}_{z2} - \sqrt{\varepsilon_{r2}}\hat{k}_{z1}\right)(\varepsilon_{r1} - \varepsilon_{r2})k_o\left(d_{\perp i}\hat{k}_{x1}\hat{k}_{x2} - d_{||i}\hat{k}_{z1}\hat{k}_{z2}\right)}{\left[\sqrt{\varepsilon_{r1}}\hat{k}_{z2} + \sqrt{\varepsilon_{r2}}\hat{k}_{z1}\right]^2 + 2\left(\sqrt{\varepsilon_{r1}}\hat{k}_{z2} + \sqrt{\varepsilon_{r2}}\hat{k}_{z1}\right)(\varepsilon_{r1} - \varepsilon_{r2})k_o\left(d_{\perp i}\hat{k}_{x1}\hat{k}_{x2} + \hat{k}_{z1}\hat{k}_{z2}\right)} \\ &\approx R_{p,F}\left\{1 + 4(\varepsilon_{r1} - \varepsilon_{r2})k_{z1}\frac{d_{\perp i}\hat{k}_{x1}^2 - d_{||i}\hat{k}_{z2}^{\ 2}}{\varepsilon_{r1}\hat{k}_{2z}^{\ 2} - \varepsilon_{r2}\hat{k}_{z1}^{\ 2}}\right\} \\ &\approx R_{p,F}\left\{1 + 4\left(n_1^2 - n_2^2\right)\frac{2\pi n_1}{\lambda_o} cos\theta_1 \frac{d_{\perp i}\sin\theta_1^2 - d_{||i}\cos\theta_2^2}{\left[n_1{}^2\cos\theta_2^2 - n_2{}^2\cos\theta_1^2\right]}\right\} \end{aligned} \tag{60}$$

$$\begin{aligned} \tau_p &\approx \frac{4\sqrt{\varepsilon_{r1}\varepsilon_{r1}}\hat{k}_{z1}\hat{k}_{z2}}{\left[\sqrt{\varepsilon_{r1}}\hat{k}_{z2} + \sqrt{\varepsilon_{r2}}\hat{k}_{z1}\right]^2 + 2(\varepsilon_{r1} - \varepsilon_{r2})k_o\left(d_{\perp i}\hat{k}_{x1}\hat{k}_{x2} + d_{||i}\hat{k}_{z2}\hat{k}_{z1}\right)\left[\sqrt{\varepsilon_{r1}}\hat{k}_{z2} + \sqrt{\varepsilon_{r2}}\hat{k}_{z1}\right]} \\ &\approx \tau_{p,F}\left[1 - 2(\varepsilon_{r1} - \varepsilon_{r2})k_o\frac{\left(d_{\perp i}\hat{k}_{x1}\hat{k}_{x2} + d_{||i}\hat{k}_{z2}\hat{k}_{z1}\right)}{\sqrt{\varepsilon_{r1}}\hat{k}_{z2} + \sqrt{\varepsilon_{r2}}\hat{k}_{z1}}\right] \\ &\approx \tau_{p,F}\left[1 - 2\left(n_1^2 - n_2^2\right)k_o\frac{\left(d_{\perp i}\sin\theta_1\sin\theta_2 + d_{||i}\cos\theta_1\cos\theta_2\right)}{\left[n_1\cos\theta_2 + n_2\cos\theta_1\right]}\right] \end{aligned} \tag{61}$$

One can of course start from approximations Eqs. (53) and (54) to obtain the same results. For absorptance from $A_p = 1 - R_p - \tau_p$, we have

$$\begin{aligned} A_p &= -\frac{4(\varepsilon_{r2} - \varepsilon_{r1})}{\left(\sqrt{\varepsilon_{r1}}\hat{k}_{z2} + \sqrt{\varepsilon_{r2}}\hat{k}_{z1}\right)^2}\mathrm{k}_{z1}\left(\hat{k}_{z2}{}^2 d_{||i} + \hat{k}_{x1}{}^2 d_{\perp i}\right) \\ &= -\frac{4\left(n_2^2 - n_1^2\right)}{\left(n_1\cos\theta_2 + n_2\cos\theta_1\right)^2}\frac{2\pi n_1}{\lambda_o}\cos\theta_1\left(d_{||i}\cos^2\theta_2 + d_{\perp i}\sin^2\theta_1\right) \end{aligned} \tag{62}$$

TE-wave. The Fresnel reflection (r_s) and transmission (t_s) coefficients for a TE-polarized incident wave are

$$r_s = \frac{\sqrt{\varepsilon_{r1}}\hat{k}_{z1} - \sqrt{\varepsilon_{r2}}\hat{k}_{z2} - ik_o d_{||}\left[\varepsilon_{r2} - \varepsilon_{r1}\right]}{\sqrt{\varepsilon_{r1}}\hat{k}_{z1} + \sqrt{\varepsilon_{r2}}\hat{k}_{z2} + ik_o d_{||}\left[\varepsilon_{r2} - \varepsilon_{r1}\right]} \tag{63}$$

$$t_s = \frac{2\sqrt{\varepsilon_{r1}}\hat{k}_{z1}}{\sqrt{\varepsilon_{r1}}\hat{k}_{z1} + \sqrt{\varepsilon_{r2}}\hat{k}_{z2} + ik_o d_{||}\left[\varepsilon_{r2} - \varepsilon_{r1}\right]} \tag{64}$$

The r_s is consistent with Eq. (32) in Schaich and Chen paper[31]. If $d_{||} = 0$, the above equations reduce to the Fresnel coefficients.

$$r_{s,F} = \frac{\sqrt{\varepsilon_{r1}}\hat{k}_{z1} - \sqrt{\varepsilon_{r2}}\hat{k}_{z2}}{\sqrt{\varepsilon_{r1}}\hat{k}_{z1} + \sqrt{\varepsilon_{r2}}\hat{k}_{z2}} = \frac{n_1 cos\theta_1 - n_2 cos\theta_2}{n_1 cos\theta_1 + n_2 cos\theta_2} \tag{65}$$

$$t_{s,F} = \frac{2\sqrt{\varepsilon_{r1}}\hat{k}_{z1}}{\sqrt{\varepsilon_{r1}}\hat{k}_{z1} + \sqrt{\varepsilon_{r2}}\hat{k}_{z2}} = \frac{2n_1 cos\theta_1}{n_1 cos\theta_1 + n_2 cos\theta_2} \tag{66}$$

We can approximate Eqs. (63) and (64) as

$$r_s \approx r_{s,F}\left[1 - \frac{2ik_{z1}d_{||}\left[\varepsilon_{r2} - \varepsilon_{r1}\right]}{\left(\sqrt{\varepsilon_{r1}}\hat{k}_{z1}\right)^2 - \left(\sqrt{\varepsilon_{r2}}\hat{k}_{z2}\right)^2}\right] \tag{67}$$

$$t_s \approx t_{s,F}\left[1 - \frac{ik_o d_{||}\left[\varepsilon_{r2} - \varepsilon_{r1}\right]}{\sqrt{\varepsilon_{r1}}\hat{k}_{z1} + \sqrt{\varepsilon_{r2}}\hat{k}_{z2}}\right] \tag{68}$$

Equation (67) is different from Eq. (4.43) in Liebsch book[15]. It seems that he had made some algebraic mistakes in his approximation. Equation (68) is consistent with Eq. (A19) in Schaich and Chen's paper[31]. However, it seems that Eq. (A20) in Schaich and Chen falls into same problem as in the Liebsch book. From these expressions, the reflectance, transmittance, and absorptance can be expressed as

$$R_s \approx R_{s,F}\left(1+\frac{4k_{z1}\left(\varepsilon_{r2}-\varepsilon_{r1}\right)}{\left(\sqrt{\varepsilon_{r1}}\hat{k}_{z1}\right)^2-\left(\sqrt{\varepsilon_{r2}}\hat{k}_{z2}\right)^2}d_{\|i}\right) = R_{s,F}\left(1+\frac{4\left(n_2^2-n_1^2\right)}{n_1^2\cos^2\theta_1-n_2^2\cos^2\theta_2}\frac{2\pi n_1}{\lambda_o}\cos\theta_1 d_{\|i}\right) \tag{69}$$

$$\tau_s=\frac{Re(k_{z2}^*)}{k_{z1}}tt^*\approx\frac{4\sqrt{\varepsilon_{r1}\varepsilon_{r2}}\hat{k}_{z1}\hat{k}_{z2}}{\left[\sqrt{\varepsilon_{r1}}\hat{k}_{z1}+\sqrt{\varepsilon_{r2}}\hat{k}_{z2}\right]^2}\left(1+\frac{2k_o d_{\|i}\left(\varepsilon_{r2}-\varepsilon_{r1}\right)}{\left[\sqrt{\varepsilon_{r1}}\hat{k}_{z1}+\sqrt{\varepsilon_{r2}}\hat{k}_{z2}\right]^2}\right) = \tau_{s,F}\left(1+\frac{2\left[n_2^2-n_1^2\right]}{n_1\cos\theta_1+n_2\cos\theta_2}\frac{2\pi}{\lambda_o}\mathrm{d}_{\|i}\right) \tag{70}$$

$$A_s=1-(R_s+\tau_s)\approx\frac{-4k_{z1}d_{\|i}\left(\varepsilon_{r2}-\varepsilon_{r1}\right)}{\left[\sqrt{\varepsilon_{r1}}\hat{k}_{z1}+\sqrt{\varepsilon_{r2}}\hat{k}_{z2}\right]^2} = \frac{-4\left[n_2^2-n_1^2\right]}{\left[n_1\cos\theta_1+n_2\cos\theta_2\right]^2}\frac{2\pi n_1}{\lambda_o}\cos\theta_1\mathrm{d}_{\|i} \tag{71}$$

In the transmittance expression, we used the Poynting vector expression for TE light $S_{i,z}=\frac{1}{2\mu\omega}\left|E_i\right|^2\mathrm{Re}\left(k_z^*\right)$. Equation (71) again shows that $d_{\|i}$ must be negative since $\varepsilon_{r2}-\varepsilon_{r1}>0$.

Power Dissipation at the Interface

The derivation below follows Liebsch's procedure[15], but arrives at the opposite sign. The surface power absorption can be calculated from

$$P(\omega)=\frac{1}{2}Re\int_{z_1}^{z_2}d\,z\boldsymbol{J}(z)\cdot\boldsymbol{E}^*(\boldsymbol{z})=\frac{\omega}{2}Im\int_{z_1}^{z_2}d\,z\boldsymbol{D}(z)\cdot\boldsymbol{E}^*(\boldsymbol{z}) \tag{72}$$

In the second step, we used the relation $\mathbf{J}=-i\omega(\boldsymbol{D}-\varepsilon_o\mathbf{E})$.

TM-polarization. For TM polarized light, Eq. (72) can be written as (see Supplementary Methods)

$$P_p(\omega)=-\frac{\omega}{2}\varepsilon_o\left(\varepsilon_{r2}-\varepsilon_{r1}\right)tt^*\left|E_i\right|^2\left[d_{\|i}cos^2\theta_2+d_{\perp i}sin^2\theta_1\right] \tag{73}$$

Dividing Eq. (73) by the Poynting vector of the incident wave in the z-direction, we get Eq. (12).

TE-Polarization. For a TE-polarized incident wave, Eq. (72) leads to

$$P_s(\omega)=-\frac{\omega}{2}\varepsilon_o\left(\varepsilon_{r2}-\varepsilon_{r1}\right)\frac{4\varepsilon_1\hat{k}_{z1}\hat{k}_{z1}}{\left[\sqrt{\varepsilon_{r1}}\hat{k}_{z2}+\sqrt{\varepsilon_{r2}}\hat{k}_{z1}\right]^2}\left|E_i\right|^2 d_{\|i} \tag{74}$$

Dividing Eq. (74) by the incident wave's Poynting vector in the z-direction, we obtain Eq. (18).

Data availability

All data are included in the manuscript.

Received: 17 May 2024; Accepted: 1 October 2024;
Published online: 10 October 2024

References

1. Tu, Y. et al. Plausible photomolecular effect leading to water evaporation exceeding the thermal limit. *Proc. Natl Acad. Sci. USA* **120**, e2312751120 (2023).
2. Lv, G., Tu, Y., Zhang, J. H. & Chen, G. Photomolecular effect: visible light interaction with air-water interface. *Proc. Natl Acad. Sci.* **121**, e2320844121 (2024).
3. Zhao, F. et al. Highly efficient solar vapour generation via hierarchically nanostructured gels. *Nat. Nanotechnol.* **13**, 489–495 (2018).
4. Zhou, X., Zhao, F., Guo, Y., Zhang, Y. & Yu, G. A hydrogel-based antifouling solar evaporator for highly efficient water desalination. *Energy Environ. Sci.* **11**, 1985–1992 (2018).
5. Ghasemi, H. et al. Solar steam generation by heat localization. *Nat. Commun.* **5**, 1–7 (2014).
6. Wang, Z. et al. Bio-inspired evaporation through plasmonic film of nanoparticles at the air–water interface. *Small* **10**, 3234–3239 (2014).
7. Tao, P. et al. Solar-driven interfacial evaporation. *Nat. Energy* **3**, 1031–1041 (2018).
8. Jackson, J. D. *Classical Electrodynamics* (Wiley, 1998).
9. Max Born & Emil Wolf. *Principles of Optics* (Pergamon, New York, 1980).
10. Alejandre, J., Tildesley, D. J. & Chapela, G. A. Molecular dynamics simulation of the orthobaric densities and surface tension of water. *J. Chem. Phys.* **102**, 4574–4583 (1995).
11. Dang, L. X. & Chang, T. M. Molecular dynamics study of water clusters, liquid, and liquid-vapor interface of water with many-body potentials. *J. Chem. Phys.* **106**, 8149–8159 (1997).
12. Ludwig, R. Water: from clusters to the bulk. *Angew. Chem. Int. Ed.* **40**, 1808–1827 (2001).
13. Shen, Y. R. & Ostroverkhov, V. Sum-frequency vibrational spectroscopy on water interfaces: polar orientation of water molecules at interfaces. *Chem. Rev.* **106**, 1140–1154 (2006).
14. Feibelman, P. J. *Surface electromagnetic fields*. *Progr. Surf. Sci.* **12**, 287–408 (1982).
15. Liebsch, A. *Electronic Excitations at Metal Surfaces* (Springer Science + Business Media, LLC, 1997).
16. Stillinger, F. H. Water revisited. *Science (1979)* **209**, 451–457 (1980).
17. Laverne, J. A. & Mozumder, A. *Concerning Plasmon excitation in liquid water*. *Radiat. Res.* **133**, 282–288 (1993).
18. Reshetnyak, I., Lorin, A. & Pasquarello, A. Many-body screening effects in liquid water. *Nat. Commun.* **14**, 2705 (2023).
19. Mcintyre, J. D. E. & Aspnes, D. E. Differential reflectance spectroscopy of very thin surface films. *Surf. Sci.* **24**, 417–434 (1971).
20. Aspnes, D. E. & Studna, A. A. Anisotropies in the above-band-gap optical spectra of cubic semiconductors. *Phys. Rev. Lett.* **54**, 1956–1959 (1985).
21. Kobayashi, N. & Horikoshi, Y. Optical investigation on growth process of GaAs during migration-enhanced epitaxy. *Jpn. J. Appl. Phys.* **28**, 1880 (1989).
22. Eryiğit, R., Marschel, P. K. & Herman, I. P. Use of surface photoabsorption to analyze the optical response of GaAs(001) surfaces. *J. Vac. Sci. Technol. A* **15**, 138–144 (1997).
23. Gerischer, H., Kolb, D. M. & Sass, J. K. The study of solid surfaces by electrochemical methods. *Adv. Phys.* **27**, 437–498 (1978).
24. Endriz, J. G. Calculation of the surface photoelectric effect. *Phys. Rev. B* **7**, 15 (1973).
25. Feibelman, P. J. Self-consistent calculation of the surface photoelectric effect. *Phys. Rev. Lett.* **34**, 1092–1095 (1975).
26. Feibelman, P. J. Exact microscopic theory of surface contributions to the reflectivity of a jellium solid. *Phys. Rev. B* **14**, 762–771 (1976).
27. Kempa, K. & Schaich, W. L. Nonlocal corrections to Fresnel optics: Model calculations from first principles for flat jellium. *Phys. Rev. B* **37**, 6711–6716 (1988).
28. Kempa, K. & Schaich, W. L. Calculation of corrections to Fresnel optics from density response. *Phys. Rev. B* **34**, 547–557 (1986).

29. Kliewer, K. L. Electromagnetic effects at metal surfaces; a nonlocal view. *Surf. Sci.* **101**, 57–83 (1980).
30. Jin, D. et al. Quantum-spillover-enhanced surface-plasmonic absorption at the interface of silver and high-index dielectrics. *Phys. Rev. Lett.* **115**, 193901 (2015).
31. Schaich, W. L. & Chen, W. Nonlocal corrections to Fresnel optics: how to extend d-parameter theory beyond jellium models. *Phys. Rev. B* **39**, 10714–10724 (1989).
32. Yang, Y. et al. A general theoretical and experimental framework for nanoscale electromagnetism. *Nature* **576**, 248–252 (2019).
33. Lai, Y. C., Chen, S. Q., Mou, L. Y. & Wang, Z. N. Nanoscale electromagnetic boundary conditions based on Maxwell's equations. *Acta Phys. Sin.* **70**, 230301 (2021).
34. Gonçalves, P. A. D. et al. Plasmon–emitter interactions at the nanoscale. *Nat. Commun.* **11**, 366 (2020).
35. Shi, B., Agnihotri, M. V., Chen, S. H., Black, R. & Singer, S. J. Polarization charge: Theory and applications to aqueous interfaces. *J. Chem. Phys.* **144**, 164702 (2016).
36. Knittl, Z. *Optics of Thin Films: An Optical Multilayer Theory* (John Wiley & Sons, 1976).

Acknowledgements

I would like to thank Dr. Guangxin Lv for the experiments data used to compare with the model and his comments on the manuscript, Professor Marin Soljacic and Dr. Thomas Christensen for discussion, and Professor Bolin Liao, Dr. Carlos Marin, Mr. James Zhang, Dr. Jiachen Li, and Dr. Rohith Mittapally for commenting on the manuscript. Discussions in the past with Professors Kris Kempa, Eli Yablonovitch, Mingda Li, Dr. Michael Landry and Dr. Chuliang Fu were also very helpful. James Zhang's question on directionally led me to emphasize the Feibelman parameters should be treated as vectors. This work is partially supported by an MIT Bose Award, MIT's Abdul Latif Jameel Water and Food Systems Lab (J-WAFS) and the MIT-UMRP program.

Author contributions

The author conceived the approach and carried out the derivations and calculations.

Competing interests

The author declares no competing interests.

Additional information

Supplementary information The online version contains supplementary material available at https://doi.org/10.1038/s42005-024-01826-z.

Correspondence and requests for materials should be addressed to Gang Chen.

Peer review information *Communications Physics* thanks ChiYung Yam and the other, anonymous, reviewers for their contribution to the peer review of this work.